analytical chemistry

pubs.acs.org/ac Article

Raman-Based Differentiation of Hemp, Cannabidiol-Rich Hemp, and Cannabis

Lee Sanchez, David Baltensperger, and Dmitry Kurouski*

Cite This: https://dx.doi.org/10.1021/acs.analchem.0c00828 Read Online

ACCESS | Metrics & More | Article Recommendations | Supporting Information

ABSTRACT: Hemp (*Cannabis sativa*) has been used to treat pain as far back as 2900 B.C. Its pharmacological effects originate from a large variety of cannabinols. Although more than 100 different cannabinoids have been isolated from *Cannabis* plants, clear physiological effects of only a few of them have been determined, including delta-9 tetrahydrocannabinol (THC), cannabidiol (CBD), and cannabigerol (CBG). While THC is an illicit drug, CBD and CBG are legal substances that have a variety of unique pharmacological properties such as the reduction of chronic pain, inflammation, anxiety, and depression. Over the past decade, substantial efforts have been made to develop Cannabis varieties that would produce large amounts of CBD and CBG. Ideally, such plant varieties should produce very little (below 0.3%) if any THC to make their cultivation legal. The amount of cannabinoids in the plant material can be determined using high performance liquid chromatography (HPLC). This analysis, however, is nonportable, destructive, and time and labor consuming. Our group recently proposed to use Raman spectroscopy (RS) for confirmatory, noninvasive, and nondestructive differentiation between hemp and cannabis. The question to ask is whether RS can be used to detect CBD and CBG in hemp, as well as enable confirmatory differentiation between hemp, cannabis, and CBD-rich hemp. In this manuscript, we show that RS can be used to differentiate between cannabis, CBD-rich plants, and regular hemp. We also report spectroscopic signatures of CBG, cannabigerolic acid (CBGA), THC, delta-9-tetrahydrocannabinolic acid (THCA), CBD, and cannabidiolic acid (CBDA) that can be used for Raman-based quantitative diagnostics of these cannabinoids in plant material.

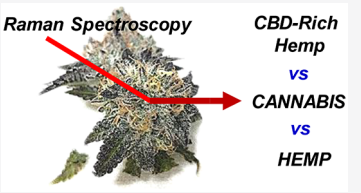

Over the past decade substantial efforts have been made to develop CBD- and CBG-rich hemp varieties.[1] After plant harvesting, these compounds can be extracted and used in a large number of commercial products ranging from oils and gums to alcoholic beverages and sprays. CBG has a large spectrum of pharmacological activity. It is known to kill or decelerate bacterial growth, reduce inflammation, and inhibit tumor cell growth.[2,3] CBG has also been found to be particularly effective in glaucoma treatment because it reduces intraocular pressure.[4]

In *Cannabis* plants, CBGA can be converted to CBD and THC, as well as the acid derivatives of these cannabinols (cannabidiolic acid (CBDA) and THCA),[5] Scheme 1. CBD relieves chronic pain, lowers blood pressure, and reduces inflammation, anxiety and depression. It can also alleviate side effects related to cancer treatment, such as nausea and vomiting.[1] Lastly, CBD is capable of mitigating symptoms of neurological disorders, such as reduction of muscle spasticity in people with multiple sclerosis.[6,7]

THC is considered to be an illicit drug due to its well-defined psychoactive properties. On a federal and state-specific level, its trafficking and possession are considered a felony offense that carries serious consequences such as prison time and significant monetary fines. Therefore, hemp farmers are constantly seeking hemp varieties that would produce high concentrations of CBD and CBG and little if any THC. Such analysis is primarily done by HPLC and mass spectrometry.[8−11] These sophisticated tests are destructive, time-consuming and can only be performed in certified laboratories. This drastically complicates hemp farming.[11]

Scheme 1. Structures of CBG-A, CBG, CBD-A, CBD, THC-A, and THC Cannabinols Present in *Cannabis* Plants

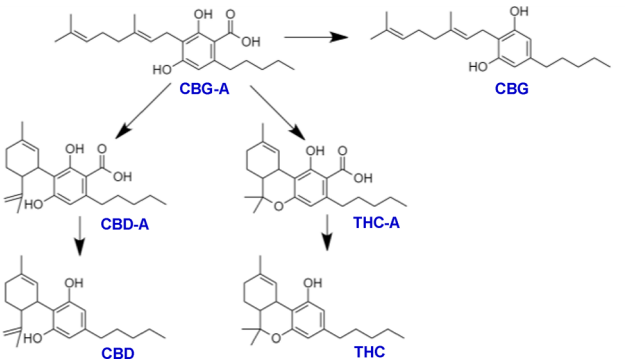

Received: February 24, 2020
Accepted: May 13, 2020
Published: May 13, 2020

Recently, our group demonstrated that cannabis/hemp diagnostics can be done by noninvasive and nondestructive spectroscopic analysis of fresh plant material.[12] Using a hand-held Raman spectrometer, we were able to distinguish hemp from cannabis with 100% accuracy, as well as differentiate three different cannabis varieties with on average 97% accuracy. Raman spectroscopy (RS) is based on inelastic light scattering of photons, which excite molecules in the sample to higher vibrational or rotational states.[9] After these inelastically scattered photons are collected by a spectrometer, the change in the photon energy is determined. Since the change in the photon energy will directly depend on the vibrational properties of molecules in the sample, RS can be used to probe structure and composition of analyzed specimens.[13]

The question to ask is whether RS can be used to distinguish between hemp, cannabis, which is used in this paper to refer to hemp plants rich in THCA, as well as CBD-rich hemp. To answer this question, we have collected Raman spectra from four different CBD-rich hemp varieties. We compared these spectroscopic signatures to the Raman spectra collected from cannabis and hemp reported in our previous study (Sanchez et al., *RSC Advances*, 2020)[12].

EXPERIMENTAL SECTION

Materials. Cannabinol standards CBG, CBGA, CBDA, THCA, and THC were received as a gift from CannID (Austin, TX). These standards were originally manufactured by Cerilliant (Round Rock, TX). Chemical structures of these compounds are shown in the Scheme 1. Solvents were evaporated from these standards by leaving uncapped vials for several hours in a fume hood. Next, residual cannabinol oils were redissolved in ethanol and deposited onto clean microscope coverslips and dried under room temperature. CBD isolate (Scheme 1) was received from Texas Farm & Process, LLC.

Plants. Hemp plants with the following amounts of THCA, CBDA, CBD, CBGA, and CBG were used: (1) "T5−005", THCA: 0.09%, THC: 0%, CBDA: 1.68%, CBD: 0.64%, CBGA: 0.1%, CBG: 0.02%; (2) "Trump sauce-006 (TS006)", THCA: 0.1%, THC: 0%, CBDA: 2.27%, CBD: 0.67%, CBGA: 0.05%, CBG: 0%; (3) "T5-Joey-008", THCA: 0.13%, THC: 0%, CBDA: 2.48%, CBD: 0.34%, CBGA: 0.15%, CBG: 0%; and (4) "Hawaii haze-010", THCA: 0.13%, THC: 0%, CBDA: 2.15%, CBD: 0.25%, CBG: 0.03%; CBGA: 0.18%. These hemp varieties have been grown on a plant farm located in Delta, CO. Spectra were collected from 10 to 15 buds of 2−3 fresh plants of each variety.

Hemp and cannabis plants were grown at Evergreen Enterprises LLC located in Denver, CO. Cannabis variety known as "twisted sherbert" (TS) contained THCA: 4.05% THCA, THC: 0.04%, CBDA: 0%, CBD: 0%, CBGA: 0.23%, CBG: 0%. Hemp contained: THCA: 0% THCA, THC: 0%, CBDA: 1.08%, CBD: 0.07%, CBGA: 0%, CBG: 0%.[12] Hemp spectra were collected from buds of 5−10 fresh plants; cannabis spectra were collected from buds of 10−15 fresh-frozen plants. Fresh-freezing of plants was performed by placement of plant buds into freezer at −10 to −15 °C. Fresh-freezing is a standard procedure in cannabis farming that is used to preserve cannabinol content of plants during their postharvest processing. Based on visual examination, fresh-freezing does not result in any noticeable changes in plant appearance or texture.

Certificates of analyses are provided in the Supporting Information.

Raman Spectroscopy. Raman spectra from plants were taken with a hand-held Resolve Agilent spectrometer equipped with 830 nm laser source (beam diameter ∼2 mm). Resolve spectral resolution was 15 cm^{-1}. Samples were brought in a direct contact with the spectrometer for spectral acquisition. The following experimental parameters were used for all collected spectra: 10s acquisition time, 495 mW power. The spectra were automatically baselined by the instrument software. In total, 20−40 spectra were collected from each sample type (hemp, CBD-rich hemp and cannabis). Spectra shown in the manuscript are raw baseline corrected, without smoothing.

Raman spectra from CBG, CBGA, CBDA, THCA, and THC oils deposited on microscope coverslips were collected on a home-built inverted microscope (Nikon TE-2000U) with 20× dry Nikon objective (NA = 0.45). A single longitudinal diode mode laser (Cobolt, Germany) was used to generate a 488 nm laser light that was directed to the microscope and reflected through 50/50 beam splitter to the sample. The scattered light was directed to a confocal IsoPlane SCT 320 Raman spectrometer (Princeton Instruments, NJ, U.S.A.) equipped with a 1200 groove/mm grating blazed at 500 nm. Prior to entering the spectrograph, Rayleigh scattering was filtered with a LP02-488RE-25 long-pass filter (Semrock, NY, U.S.A.). The spectrograph dispersed light was then sent to PIXIS:400BR CCD (Princeton Instruments, NJ, USA). A motorized stage H117P2TE (Prior, MA, U.S.A.) controlled by Prior Proscan II was used to move the sample relative to the incident laser beam. Raman spectrum from CBD isolate was collected using a hand-held Resolve Agilent spectrometer. All data were processed using GRAMS/AI 7.0 (Thermo Galactic, NH, U.S.A.).

Multivariate Data Analysis. SIMCA 14 (Umetrics, Umeå, Sweden) was utilized for statistical data treatment of the Raman spectra collected in this study. Imported spectra were truncated so as to only include wavenumbers 701−1700 cm^{-1} and scaled to unit variance via standard normal variate (SNV) correction in order to give all spectral regions equal importance. Spectra were then normalized by the total area followed by a first derivative application. classes. Next, with orthogonal partial least-squares discriminant analysis (OPLS-DA), we determined the number of predicting and orthogonal significant components and identified spectral regions that best explain the separation between the classes.

RESULTS AND DISCUSSION

Raman spectra of CBD-rich hemp (for clarity, spectra of only T5-005 and TS006 are shown in Figure 1) exhibited vibrational bands that can be assigned to cellulose, xylan, carotenoids, and lignin, Figure 1 and Table 1.[14] These vibrational bands were also present in the spectra of hemp and cannabis (TS). We have found substantial difference in the intensities of vibrational bands of cellulose and carotenoids in these three groups of plants. Specifically, T5-005 and TS006 exhibited the highest intensity of a vibrational band at 1525 cm^{-1}, which can be assigned to carotenoid. At the same time, intensity of this band is lower in the spectrum of hemp and cannabis. Similar changes have been observed for vibrational bands at 1155−1228 cm^{-1}, which can be assigned to cellulose and xylan. These spectral changes suggest a substantial difference in scaffold molecules in hemp, cannabis, and

https://dx.doi.org/10.1021/acs.analchem.0c00828
Anal. Chem. XXXX, XXX, XXX−XXX

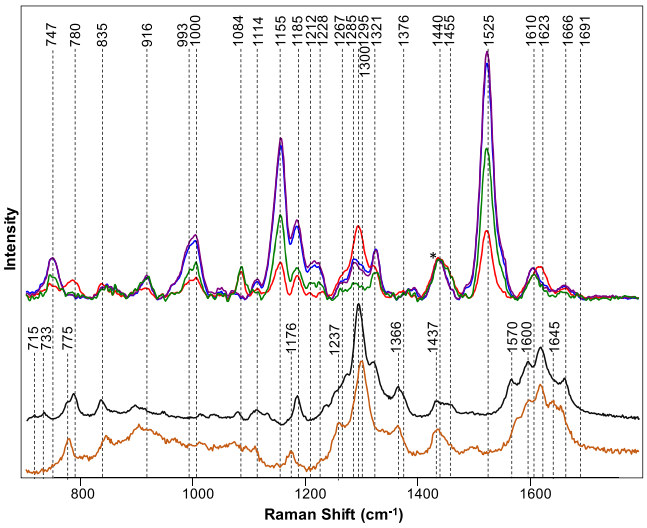

Figure 1. Top: Raman spectra collected form T5−005 (purple) and TS006 (blue), hemp (green) and TS (red). Bottom: Raman spectra of THCA (black) and CBDA (orange). Spectra normalized on CH_2 vibrations (1440 cm^{-1}) that are present in nearly all classes in biological molecules (marked by asterisks (*)).

Table 1. Vibrational Bands and Their Assignments for Hemp, Cannabis Species, and THCA

band	vibrational mode	assignment
780	TBA	cannabinoids[12]
835	TBA	cannabinoids[12]
916	ν(C−O−C) in plane, symmetric	cellulose, lignin[15]
993−1000	ν3 (C−CH3 stretching) and phenylalanine	carotenoids, protein[16,17]
1084	ν(C−O)+ν(C−C)+δ(C−O−H)	carbohydrates[18]
1114	νsym(C−O−C), C−OH bending	cellulose[19,20]
1155	νasym(C−C) ring breathing	carbohydrates, cellulose[15]
1185	ν(C−O−H) next to aromatic ring+σ(CH)	xylan[21,22]
1212−1228	δ(C−C−H)	aliphatic,[23] xylan[21]
1267	C−O stretching (aromatic)	lignin[24]
1285	δ(C−C−H)	aliphatic[23]
1295	TBA	cannabinoids[12]
1321	δCH2 bending vibration	cellulose, lignin[15]
1376	δCH2 bending vibration	aliphatic[23]
1440	δ(CH2) + δ(CH3)	aliphatic[23]
1455	δCH2 bending vibration	aliphatic[23]
1525	—C═C— (in plane)	carotenoids[25,26]
1610	ν(C−C) aromatic ring +σ(CH)	lignin[27,28]
1623−1666	aromatic	cannabinoids[12,29]

CBD-rich plants. Such changes can be used to identify plant varieties or even predict geographical origin of their growth.

We have also observed substantial differences in the vibrational bands that can be assigned to THCA in hemp, cannabis, and CBD-rich plants. As was previously discussed, TS exhibits vibrational bands at 780, 1295, 1623, and 1666 cm^{-1}, which can be assigned to THCA. We have not observed vibrational bands at 780 and 1623 cm^{-1} in the spectra of T5-005 and TS006, whereas the intensity of 1666 cm^{-1} band was nearly identical as in the spectrum of TS. Thus, this spectral difference can be used to distinguish between CBD-rich hemp and cannabis. At the same time, we have observed an increased intensity of vibrational bands at 1295−1300 cm^{-1} in the

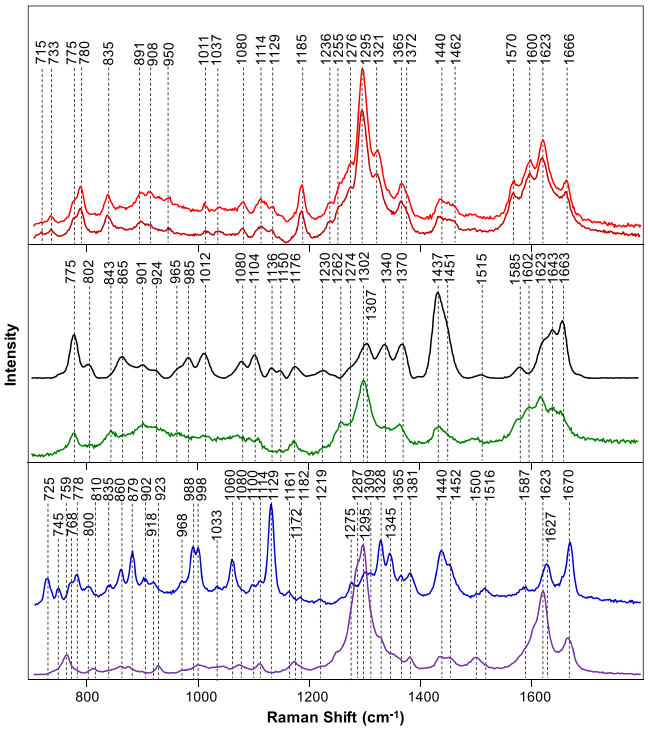

Figure 2. Raman spectra of THC (red), THCA (maroon), CBD (black), CBDA (green), CBG (blue), and CBGA (violet).

Table 2. Vibrational Bands Observed in the Raman Spectra of THC, THCA, CBD, CBDA, CBG, and CBGA

compound	vibrational bands, cm^{-1}
THC	733, 775, 780, 835, 891, 908, 950, 1011, 1037, 1080, 1114, 1129, 1185, 1236, 1255, 1276, 1295, 1321, 1365, 1372, 1440, 1462, 1570, 1600, 1623, 1666
THCA	715, 733, 775, 780, 835, 891, 908, 950, 1011, 1037, 1080, 1114, 1129, 1185, 1236, 1255, 1276, 1295, 1321, 1365, 1372, 1440, 1462, 1570, 1600, 1623, 1666
CBD	775, 802, 865, 901, 924, 965, 985, 1012, 1080, 1104, 1136, 1150, 1176, 1230, 1262, 1274, 1302, 1340, 1370, 1437, 1451, 1515, 1585, 1623, 1643, 1663
CBDA	775, 802, 843, 901, 1176, 1262, 1307, 1370, 1437, 1451, 1585, 1602, 1623, 1643, 1663
CBG	725, 745, 768, 778, 800, 810, 835, 860, 879, 902, 918, 968, 988, 998, 1033, 1060, 1100, 1114, 1129, 1161, 1182, 1219, 1275, 1295, 1309, 1328, 1345, 1365, 1381, 1440, 1452, 1516, 1587, 1623, 1627, 1670
CBGA	759, 810, 860, 879, 923, 998, 1080, 1114, 1172, 1287, 1295, 1381, 1440, 1452, 1500, 1623, 1670

Table 3. Accuracy of Classification by OPLS-DA for Cannabis, Industrial, and CBD-Rich Hemp

	members	correct	hemp	cannabis	CBD-risch hemp
hemp	22	100%	22	0	0
cannabis	64	100%	0	64	0
CBD-rich hemp	126	100%	0	0	126
Fisher's prob.	9.3×10^{-12}				

spectra of T5−005 and TS006 relative to the intensities of these bands in the spectra of hemp. This spectral difference can be used to enable confirmatory differentiation between industrial hemp and CBD-rich hemp.

Although spectroscopic analysis of plant material reveals striking differences between cannabis and CBD-rich hemp, Raman signatures of THCA and CBDA are very similar.

https://dx.doi.org/10.1021/acs.analchem.0c00828
Anal. Chem. XXXX, XXX, XXX−XXX

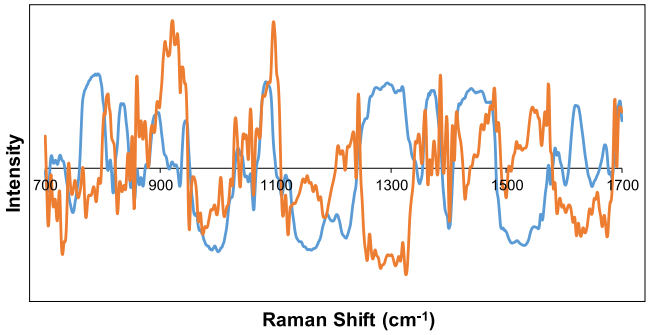

Figure 3. Loading plot of two predictive components (component 1 (blue) and component 2 (orange)) in the Raman spectra of cannabis, hemp, and CBD-rich hemp.

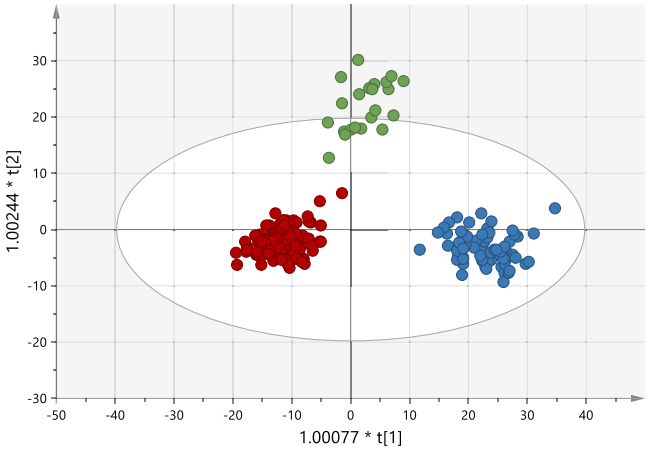

Figure 4. OPLS-DA variant component plot of Raman spectra collected from hemp (green), cannabis (blue), and CBD-rich hemp (red).

THCA and CBDA exhibit very similar structures (Scheme 1), consequently reflected in the profiles of vibrational bands in 1570−1691 and 1212−1366 cm^{-1} spectral regions. At the same time, we found that THCA has a vibrational band centered at 1295 cm^{-1}, which has been found to be 5 cm^{-1} red-shifted in the spectrum of CBDA. Also, Raman spectrum of THCA exhibits a vibrational band at 1185 cm^{-1}, which was not evident in the spectrum of CBDA. Raman spectrum of THCA has a doublet at 775 and 780 cm^{-1}, whereas only one vibrational band at 775 cm^{-1} has been detected in the spectrum of CBDA. The spectroscopic analysis of vibrational bands of THCA and CBDA suggests that only the band at 780 cm^{-1} can be used for confirmatory differentiation between THCA and CBDA. One can also envision that an intensity of the vibrational band at 1623 cm^{-1} is present in the spectrum of cannabis (4.05% of THCA) and absent in the spectrum of CBD-rich hemp (T5−005; CBDA 1.68%, TS006; CBDA 2.27%) due to differences in the amount of THCA and CBDA in these two groups of plants. Alternatively, such difference in the intensity of 1623 cm^{-1} can be attributed to the difference in the Raman cross-section of these THCA and CBDA. Additional studies are required to fully elucidate Raman cross sections of THCA and CBDA to enable quantitative prediction of their content in plants.

The question to ask is how different are the spectroscopic signatures of CBDA and THCA from their decarboxylated derivatives. We found that THCA and THC exhibit nearly identical Raman spectra, Figure 2. These results suggest that both THCA and THC can be detected in the plant using RS. We have also observed high similarity between spectra collected from CBDA and CBD. Both spectra exhibited vibrational bands at 775, 802, 901, 1176, 1370, 1437, 1585, 1623, 1643, and 1663 cm^{-1}. However, CBD had peaks at 865, 985, 1080, 1104, 1136, 1150, 1274, and 1515 cm^{-1} that were not observed in the spectra of CBDA. At the same time, CBDA has peaks at 843, 1262, and 1602 cm^{-1} that were not observed in the spectrum of CBD. We have also observed that a peak centered at 1307 in the spectrum of CBD was 5 cm^{-1} blue-shifted in the spectrum of CBDA.

Interestingly, CBGA and CBG exhibited greater spectroscopic difference relative to those observed between THCA and THC, as well as between CBDA and CBD, Figure 2. Although nearly all vibrational bands were present in both CBGA and CBG spectra, their relative intensities were drastically different, Figure 2 and Table 2. For instance, vibrational bands at 1287−1295 cm^{-1} were found to be the most intense in the spectrum of CBGA. However, the band centered at 1129 cm^{-1} were the most intense in the spectrum of CBG. It should be noted that this band was not present in the spectrum of CBGA.

Although hemp plants typically have very small quantities of CBG/CBGA ("T5-005"; CBGA: 0.1%, CBG: 0.02%; 'TS006', CBGA: 0.05%, CBG: 0%), our results demonstrate that RS can be used for identification of this cannabinol in CBG/CBGA-rich hemp. Specifically, we found that bands at 725−768, 879, 998, and 1060 cm^{-1} are unique for CBG/CBGA and are not present in the Raman spectra of THC/THCA and CBD/CBDA.

To further prove our expectation that RS can be used for highly accurate differentiation between hemp, CBD-rich hemp, and cannabis, we used OPLS-DA analysis. The final model, containing one predictive component, 2 orthogonal components, and 1001 (701−1700 cm^{-1}) out of 1651 original wavenumbers, was used to generate the misclassification table (Table 3) and the loadings plot (Figure 3). It should be noted that for the reported OPLS-DA model, in addition to the Raman spectra of TS, we have used spectra collected from two other cannabis varieties known as "triple chocolate chip (TCC)" and "gelato cake (GC)". Detailed spectroscopic analysis of these cannabis varieties, as well as their cannabinoid profiles have been previously reported by our group study (Sanchez et al., RCS Advances, 2020). The spectra of GC and TCC have been included in the reported model to increase the number of Raman spectra of cannabis.

The first predictive component (PC; Figure 3) explains 92% of the variation between classes. Absolute intensities in the loading spectrum are proportional to the percentage of the total variation between classes explained by each wavenumber. The model identified the peak at 780 cm^{-1}, which could be assigned to cannabinoids (Table 1), cellulose, and lignin peaks at ~916 cm^{-1} and the bands at 1260−1321 cm^{-1}, which correspond to both THCA and cellulose. Also, the model identified peaks at 1440 cm^{-1}, which could be assigned to aliphatic vibrations and bands at 1623−1666 cm^{-1}, which originate from cannabinoids, to be the strongest spectral markers of cannabis, which supports the conclusions of our qualitative spectral analysis above. This indicates that coupling of OPLS-DA with RS allows for a 100% accurate differentiation between cannabis, hemp and CBD-rich hemp, Tables 3 and 4.

https://dx.doi.org/10.1021/acs.analchem.0c00828
Anal. Chem. XXXX, XXX, XXX−XXX

CONCLUSIONS

Our results clearly demonstrate that RS can be used for confirmatory, noninvasive, and nondestructive differentiation between hemp, CBD-rich hemp, and cannabis (THCA-rich hemp) with 100% accuracy. We also reported Raman spectra of six major cannabinoids, THC, THCA, CBD, CBDA, CBG, and CBGA. Analysis of their vibrational fingerprint shows that RS can be used for identification of these chemicals in plant material. We also provided experimental evidence that allows for differentiation between THC/THCA vs CBD/CBDA vs CBG/CBGA, as well as between CBD-CBDA and CBG-CBGA. These results substantially expand applicability of RS as a tool for hemp cultivation and breeding.

ASSOCIATED CONTENT

Supporting Information

The Supporting Information is available free of charge at https://pubs.acs.org/doi/10.1021/acs.analchem.0c00828.

HPLC results of cannabis analyses that demonstrate cannabinoid content of analyzed plant material (PDF)

AUTHOR INFORMATION

Corresponding Author

Dmitry Kurouski − *Department of Biochemistry and Biophysics and The Institute for Quantum Science and Engineering, Texas A&M University, College Station, Texas 77843, United States;* orcid.org/0000-0002-6040-4213; Phone: 979-458-3778; Email: dkurouski@tamu.edu

Authors

Lee Sanchez − *Department of Biochemistry and Biophysics, Texas A&M University, College Station, Texas 77843, United States*

David Baltensperger − *Department of Soil and Crop Sciences, Texas A&M University, College Station, Texas 77843, United States*

Complete contact information is available at: https://pubs.acs.org/10.1021/acs.analchem.0c00828

Notes

The authors declare no competing financial interest.

ACKNOWLEDGMENTS

We are grateful to Cree Crawford, Co-Founder and President of Cann-ID, as well as to all members of this company for providing cannabinoid standards. We are also trateful to Conor Filter and Haden Shibley for the provided access to help and cannabis plants, as well as for providing CBD isolate. We are grateful to AgriLife Research of Texas A&M for the provided financial support. We also acknowledge Governor's University Research Initiative (GURI) grant program of Texas A&M University, GURI Grant Agreement No. 12-2016, M1700437.

REFERENCES

(1) Hartsel, J. A.; Eades, J.; Hickory, B.; Makriyannis, A. *Nutraceuticals* **2016**, 735−754.

(2) Appendino, G.; Gibbons, S.; Giana, A.; Pagani, A.; Grassi, G.; Stavri, M.; Smith, E.; Rahman, M. M. *J. Nat. Prod.* **2008**, *71* (8), 1427−30.

(3) Borrelli, F.; Fasolino, I.; Romano, B.; Capasso, R.; Maiello, F.; Coppola, D.; Orlando, P.; Battista, G.; Pagano, E.; Di Marzo, V.; Izzo, A. *Biochem. Pharmacol.* **2013**, *85* (9), 1306−16.

(4) Nadolska, K.; Gos, R. *Klin Oczna* **2008**, *110* (7−9), 314−7.

(5) Havelka, J. What is CBG (cannabigerol) & what does this cannabinoid do? *Leafly*, 2017; https://www.leafly.com/news/cannabis-101/what-is-cbg-cannabinoid, accessed March 2020.

(6) Mouslech, Z.; Valla, V. *Neuro. Endocrinol. Lett.* **2009**, *30* (2), 153−79.

(7) Darkovska-Serafimovska, M.; Serafimovska, T.; Arsova-Sarafinovska, Z.; Stefanoski, S.; Keskovski, Z.; Balkanov, T. *J. Pain Res.* **2018**, *11*, 837−842.

(8) Burnier, C.; Esseiva, P.; Roussel, C. *Talanta* **2019**, *192*, 135−141.

(9) Zivovinovic, S.; Alder, R.; Allenspach, M. D.; Steuer, C. *J. Anal. Sci. Technol.* **2018**, *9*, 1−10.

(10) Patel, B.; Wene, D.; Fan, Z. T. *J. Pharm. Biomed. Anal.* **2017**, *146*, 15−23.

(11) Nie, B.; Henion, J.; Ryona, I. *J. Am. Soc. Mass Spectrom.* **2019**, *30* (5), 719−730.

(12) Sanchez, L.; Filter, C.; Baltensperger, D.; Kurouski, D. *RSC Adv.* **2020**, *10*, 3212−3216.

(13) Farber, C.; Mahnke, M.; Sanchez, L.; Kurouski, D. *TrAC, Trends Anal. Chem.* **2019**, *118*, 43−49.

(14) Sanchez, L.; Ermolenkov, A.; Tang, X. T.; Tamborindeguy, C.; Kurouski, D. *Planta* **2020**, *251*, 64.

(15) Edwards, H. G.; Farwell, D. W.; Webster, D. *Spectrochim. Acta, Part A* **1997**, *53A* (13), 2383−92.

(16) Tschirner, N.; Brose, K.; Schenderlein, M.; Zouni, A.; Schlodder, E.; Mroginski, M. A.; Hildebrandt, P.; Thomsen, C. *Phys. Status Solidi B* **2009**, *246* (11−12), 2790−2793.

(17) Kurouski, D.; Van Duyne, R. P.; Lednev, I. *Analyst* **2015**, *140* (15), 4967−80.

(18) De Gussem, K.; Vandenabeele, P.; Verbeken, A.; Moens, L. *Spectrochim. Acta, Part A* **2005**, *61* (13−14), 2896−2908.

(19) Edwards, H. G. M.; Farwell, D. W.; Webster, D. *Spectrochim. Acta, Part A* **1997**, *53* (13), 2383−2392.

(20) Agarwal, U. P.; Ralph, S. A. *Appl. Spectrosc.* **1997**, *51* (11), 1648−1655.

(21) Agarwal, U. *Front. Plant Sci.* **2014**, *5*, 1−12.

(22) Mary, Y. S.; Panicker, C. Y.; Varghese, H. *Orient. J. Chem.* **2012**, *28* (2), 937−941.

(23) Yu, M. M.; Schulze, H. G.; Jetter, R.; Blades, M. W.; Turner, R. *Appl. Spectrosc.* **2007**, *61* (1), 32−7.

(24) Cao, Y.; Shen, D.; Lu, Y.; Huang, J. *Ann. Bot.* **2006**, *97*, 1091−1094.

(25) Devitt, G.; Howard, K.; Mudher, A.; Mahajan, S. *ACS Chem. Neurosci.* **2018**, *9*, 404.

(26) Adar, F. *Spectroscopy* **2017**, *32* (6), 12−20.

(27) Kang, L.; Wang, K.; Li, X.; Zou, B. *J. Phys. Chem. C* **2016**, *120* (27), 14758−14766.

(28) Agarwal, U. *Planta* **2006**, *224* (5), 1141−53.

(29) Sivashanmugan, K.; Squire, K.; Tan, A.; Zhao, Y.; Kraai, J. A.; Rorrer, G. L.; Wang, A. *ACS Sens.* **2019**, *4* (4), 1109−1117.